X-671-65-244

NASA T-M X-55235

NEWTONIAN AERODYNAMICS FOR TANGENT OGIVE BODIES OF REVOLUTION

BY
EDWARD E. MAYO

JUNE 1965

NASA
GODDARD SPACE FLIGHT CENTER
GREENBELT, MARYLAND

X-671-65-244

NEWTONIAN AERODYNAMICS FOR TANGENT OGIVE BODIES OF REVOLUTION

by

Edward E. Mayo

June 1965

Goddard Space Flight Center
Greenbelt, Maryland

CONTENTS

NEWTONIAN AERODYNAMICS FOR TANGENT OGIVE BODIES OF REVOLUTION

by

Edward E. Mayo

ABSTRACT

Aerodynamic coefficients and static stability characteristics of tangent ogive bodies of revolution are presented. The body fineness ratio varied from a hemisphere (fineness ratio = 0.5) to a fineness ratio of 7 and the angle of attack ranged from 0 to 180°.

NEWTONIAN AERODYNAMICS FOR TANGENT OGIVE BODIES OF REVOLUTION

by

Edward E. Mayo

SUMMARY

30185

Aerodynamic coefficients and static stability characteristics of tangent ogive bodies of revolution are presented. The body fineness ratio varied from a hemisphere (fineness ratio = 0.5) to a fineness ratio of 7 and the angle of attack ranged from 0 to 180 degrees. Since, for most applications, an afterbody will be added to the tangent ogive to form a complete vehicle, the aerodynamics presented do not include the effects of the base.

An increase in fineness ratio resulted in increased lift, decreased drag and, subsequently, a rapid increase in the lift-to-drag ratio. Near zero lift, the agreement between the impact theory and existing experimental stability values improves with increasing Mach number with the exception of the normal force derivative for fineness ratios less than 4. The axial force coefficient is not adequately predicted by the impact theory, particularly at low angles of attack where the skin friction and base drag become significant contributors to the total drag.

Author

SYMBOLS

C_A	axial force, force coefficient, axial force/qS
C_D	drag force coefficient, drag force/qS
C_L	lift force coefficient, lift force/qS
C_m	pitching moment coefficient, pitching moment/qSD
C_N	normal force coefficient, normal force/qS
C_{N_α}	$\frac{\Delta C_N}{\Delta \alpha}_{\alpha = 0,5^\circ}$
d	reference diameter
f	fineness ratio, ℓ/d
ℓ	body length
L/D	lift-drag ratio
M	free stream Mach number
q	dynamic pressure
R_N	free stream Reynolds number based on configuration length
S	reference area, $\frac{\pi d^2}{4}$
S_W	wetted area
x_{cp}	center-of-pressure location, aft of nose,
α	angle-of-attack, deg.
δ	surface slope from body axis, $\delta(x/d)$
ρ	radius vector for cylindrical coordinates, $\rho(x/d)$

NEWTONIAN AERODYNAMICS FOR TANGENT OGIVE BODIES OF REVOLUTION

INTRODUCTION

In modifying the known zero lift aerodynamics for vehicles with tangent ogive noses to correspond to other configurations, the tangent ogive aerodynamics must be known. The available methods of prediction are limited to small angles of attack. For cases where it is desirable to know the aerodynamics at large angles of attack (for example, in determining payload dynamics during re-entry), there is insufficient experimental data and no eloquent means of theoretical prediction.

In reference 1, experimental tests at Mach numbers from 2.75 to 5.0 at angles of attack up to 25° showed that with increasing Mach number the aerodynamic characteristics of fineness ratio 3, 5 and 7 tangent ogives approached those predicted by Newtonian Impact theory. Thus, it may be surmised that for the lower supersonic or lower hypersonic (depending upon the fineness ratio) Mach numbers, the second order shock expansion theory of reference 2 would adequately predict the near zero lift aerodynamics; and at the higher Mach numbers, the Impact theory should yield adequate preliminary prediction. Based on the studies of reference 3, and experimental programs supporting reference 4, the Impact theory (or modified Impact theory) should also yield adequate prediction at the large angles of attack. As the angle of attack is increased, it is anticipated that the agreement Mach number will decrease since the hypersonic similarity parameter ($M\delta$) , more or less, determines the agreement Mach number.

The closed form solutions for the prediction of the Newtonian Impact aerodynamics for tangent ogive bodies at high angles of attack probably would require more time to evaluate than the basic integrals themselves. References 4 and 5 have shown that the machine computation of the Newtonian aerodynamics according to the procedures given in reference 5 is extremely accurate. The computer solution time is on the order of several minutes for a complete angle-of-attack range. The computer program of reference 5 was used to generate the coefficients presented herein.

The purpose of this paper is to present the Newtonian static aerodynamic characteristics for tangent ogive bodies at angles of attack from 0° to 180°. Particular emphasis has been given to the comparison of the fineness ratio 3, 5 and 7 bodies with existing experimental data.

CONFIGURATION AND RANGE OF VARIABLES

The tangent ogive configuration and aerodynamic reference system used herein is shown in Figure 1. Computations were performed for body fineness ratios of 0.5 and 1 to 7 in unit increments. The angle of attack varied from 0° to 10° in 1° increments; from 10° to 30° in 2.5° increments; and from 30° to 180° in 5° increments.

METHOD OF COMPUTATION

All aerodynamic coefficients presented were determined by numerically integrating the Newtonian force and moment equations of reference 5 on an IBM 7094 digital computer. The tangent ogive body geometry, as shown in Figure 1, was programmed into the body coefficient expressions of reference 5. The body equations for the tangent ogive are derived in the Appendix and summarized below.

$$\frac{\rho}{d} = \sqrt{(f^2 + 1/4)^2 - (x/d - f)^2} - (f^2 - 1/4)$$

$$\delta = \tan^{-1}\left[\frac{f - x/d}{\rho/d + f^2 - 1/4}\right]$$

All coefficients correspond to a maximum stagnation point pressure coefficient of 2.* Since, for most applications, an afterbody will be added to the tangent ogive to form a complete vehicle, the aerodynamics presented do not include the effects of the base. The center-of-pressure location and normal force coefficient curve slope near zero angle of attack were determined by assuming linearity from 0 to 5 degrees angle of attack.

*All the computed coefficients may be modified to correspond to the actual stagnation point pressure coefficient by multiplying the computed coefficients by the ratio of the actual stagnation point pressure coefficient to the Newtonian value (2.0).

RESULTS AND DISCUSSION

For convenience of the user, the aerodynamic coefficients are presented in both tabular and graphical form.* The basic aerodynamics are given in Table 1 and Figure 2. It is seen from figures 2(d), 2(e), and 2(f) that near zero lift, an increase in fineness ratio results in increased lift, decreased drag, and subsequently, a rapid increase in lift-to-drag ratio.

In Figure 3, the near zero lift stability characteristics are compared with the experimental values given in reference 2. The agreement between the impact theory and experimental stability values improves with increasing Mach number with the exception of the normal force derivative for fineness ratios less than about 4.

A comparison of the impact theory for fineness ratio 3, 5 and 7 bodies with experimental values from reference 1 is presented in Figure 4.** In general, as previously substantiated in reference 1, Figure 4 shows that with increasing Mach number the aerodynamic characteristics approach those predicted by Newtonian impact theory.

The axial force coefficient is not adequately predicted by the impact theory, particularly at the lower angles of attack where the skin friction and base drag contributions become significant contributors to the total drag. As the angle of attack and Mach number is increased, the agreement between the impact theory and axial force coefficients improves. (Omitting M = 5 data in which possible air condensation effects exists.) To gain an insight into the magnitude of the various contributors to the axial force at zero angle of attack, the skin friction (assuming completely laminar and completely turbulent flow over the entire model) and base drag (assuming a turbulent boundary layer ahead of the base) were determined. The skin friction contribution was determined via reference 6. In reference 6, the average flat plate friction coefficients based on wetted area as a function of Reynolds number for various Mach numbers are given. (For the values computed herein, the flat plate values were applied directly to the tangent ogives since the indicated approximate correction factors are 16, 10 and 7 percent, respectively, for the f = 3, 5 and 7 bodies.) The ratio of the body wetted area (S_w) to the reference area (S) for tangent ogives may be expressed in terms of the body fineness ratio (f) as

---

*All of the figures presented herein, with the exception of Figures 1 and 3, were mechanically plotted. The plotter assumed linearity between the computed values presented in Table 1.

**An uncertainty exists in the M = 5 data due to the presence of a small amount of condensed air in the stream. See reference 1.

$$\frac{S_w}{S} = 8(f^2 + 1/4)^2 \left\{ \sin\left[\tan^{-1}\left(\frac{f}{f^2 - 1/4} \right) \right] - \left(1 - \frac{1}{2f^2 + 0.5} \right) \tan^{-1}\left(\frac{f}{f^2 - 1/4} \right) \right\}$$

The resulting values for S_w/S for fineness ratio 3, 5 and 7 bodies are 8.1, 13.4 and 18.7, respectively. The base drag values were obtained from references 7 and 8. The following table summarizes the various drag contributions under the aforementioned assumptions.

M	R_N	f \ C_D	Newtonian	Laminar Skin Friction	Turbulent Skin Friction	Base*	Experimental**
2.75	3.4×10^6	3	.071	.005	.021	.095	.108
		5	.026	.009	.035	.095	.053
		7	.014	.012	.049	.095	.037
4.01	3.6×10^6	3	.071	.005	.018	.065	.103
		5	.026	.008	.030	.065	.048
		7	.014	.012	.041	.065	.048
5.0	$.9 \times 10^6$	3	.071	.009	.020	.048	.110
		5	.026	.015	.034	.048	.052
		7	.014	.021	.047	.048	.040

*Turbulent flow ahead of base.
**Reference 1.

Unfortunately, base pressures were not obtained in the tests of reference 1, and the test Reynolds numbers were in the region of boundary layer transition. These factors, coupled with possible air condensation effects in the M = 5 data makes it impossible to assess the axial force prediction near zero lift. However, a comparison of the Newtonian values with pressure drag predictions from more exact theories showed that the Newtonian values were approached with increasing Mach number. For the limiting case of the hemisphere, the measured pressures at M = 4.95 reported in reference 9 agreed very well with those of the modified Newtonian theory.

The lift, drag, and lift-to-drag ratio comparisons presented in Figure 4 are not discussed since these coefficients are determined from the basic normal force and axial force coefficients previously discussed. However, it should be noted, as observed in reference 1, that the Newtonian drag coefficient distribution adequately predicts the drag trends. Thus, the drag coefficients may be determined by singularly evaluating the total drag at $\alpha = 0°$ (using the known flight conditions) and assuming a Newtonian distribution to obtain the values at angle of attack.

CONCLUDING REMARKS

Newtonian aerodynamics are presented for fineness ratio 0.5 to 7 tangent ogive bodies of revolution at angles of attack from 0 to 180°. A comparison of the generated coefficients with existing wind tunnel data lead to the following conclusions.

1. An increase in fineness ratio resulted in increased lift, decreased drag and subsequently, a rapid increase in lift-to-drag ratio.

2. Near zero lift, the agreement between the impact theory and experimental stability values improves with increasing Mach number with the exception of the normal force derivative for fineness ratios less than 4.

3. The axial force coefficient is not adequately predicted by the impact theory, particularly at low angles of attack where the skin friction and base drag become significant contributors to the total drag.

4. The Newtonian drag coefficient distribution adequately predicts the experimental drag trends. Thus, the drag characteristics may be predicted by singularly evaluating the total drag at $\alpha = 0°$ (using the known flight conditions) and assuming a Newtonian distribution to obtain the values at angle of attack.

APPENDIX

TANGENT OGIVE BODY EQUATIONS

This appendix presents the derivation of the body equations programmed into the body coefficient expressions of reference 5. The tangent ogive semi-cross section is shown encompassed by its arc circle (primed coordinates), as the cross hatched area in sketch (a).

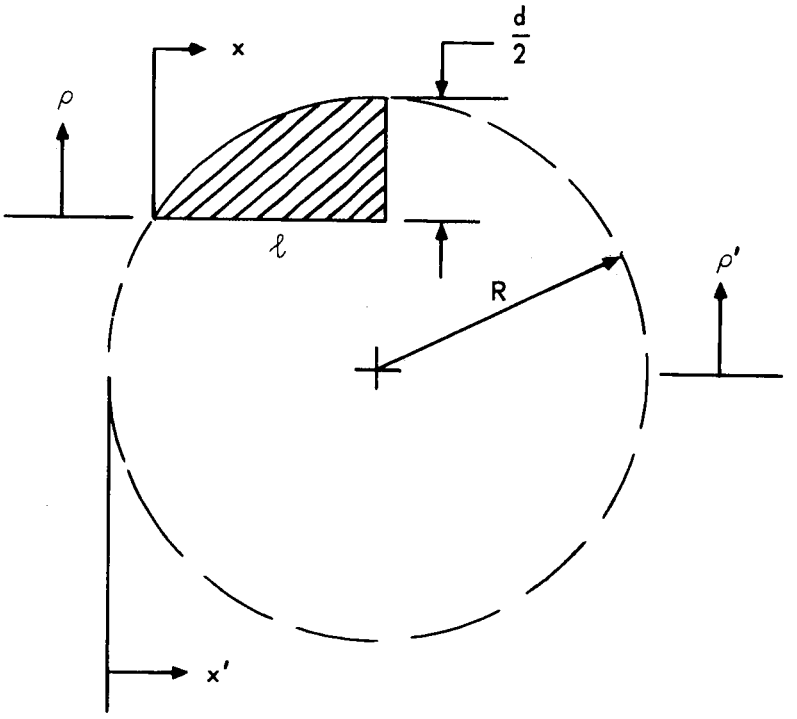

Sketch (a)

The equation of the arc circle in the primed coordinate system is given by

$$(x' - R)^2 + \rho'^2 = R^2 \qquad (1)$$

The following relationships exist between the arc circle and the ogive coordinate systems:

$$x' = x + (R - \ell) \tag{2(a)}$$

$$\rho' = \rho + (R - d/2) \tag{2(b)}$$

Substitution of equations 2(a) and 2(b) into equation (1) and nondimentionalizing, yields

$$[x/d - f]^2 + [\rho/d + (R/d - 1/2)]^2 = (R/d)^2 \tag{3}$$

which, upon solving for ρ/d, gives

$$\rho/d = \sqrt{(R/d)^2 - (x/d - f)^2} - (R/d - 1/2)$$

Making use of the relation

$$(R/d)^2 = f^2 + (R/d - 1/2)^2 \tag{4}$$

leads to the following expression for ρ/d:

$$\rho/d = \sqrt{(f^2 + 1/4)^2 - (x/d - f)^2} - (f^2 - 1/4) \tag{5}$$

The surface slope, δ, is given by

$$\delta = \tan^{-1} \frac{d(\rho/d)}{d(x/d)} \tag{6}$$

Differentiation of equation (3) according to equation (6), and making use of equation (4), yields the following relation for δ

$$\delta = \tan^{-1}\left[\frac{f - (x/d)}{\rho/d + f^2 - 1/4}\right] \tag{7}$$

Equations (5) and (7) were programmed into the body coefficient equations of reference 5 to yield the generated coefficients presented herein.

REFERENCES

1. Dennis, David H., and Cunningham, Bernard E.: Forces and Moments on Pointed and Blunt-Nosed Bodies of Revolution at Mach Numbers from 2.75 to 5.00. NACA RM A52E22, 1952.

2. Syverston, Clarence A., and Dennis, David H.: A Second-Order Shock-Expansion Method Applicable to Bodies of Revolution Near Zero Lift. NACA Report 1328, 1957.

3. Penland, Jim A.: Aerodynamic Characteristics of a Circular Cylinder at Mach Number 6.86 and Angles of Attack Up to 90°. NACA TN 3861, 1957.

4. Mayo, Edward E., Lamb, Robert H., and Romere, Paul O.: Newtonian Aerodynamics for Blunted Raked-Off Circular and Raked-Off Elliptical Cones. NASA TN D-2624, 1965.

5. Ried, Robert C., Jr. and Mayo, Edward E.: Equations for the Newtonian Static and Dynamic Aerodynamic Coefficients for a Body of Revolution with an Offset Center-of-Gravity. NASA TN D-1085, 1963.

6. Stoney, William E., Jr.: Collection of Zero-Lift Drag Data on Bodies of Revolution From Free-Flight Investigations. NASA TR R-100, 1961.

7. Love, Eugene S.: Base Pressure at Supersonic Speeds on Two-Dimensional Airfoils and on Bodies of Revolution With and Without Fins Having Turbulent Boundary Layers. NACA TN-3819, 1957.

8. John Hopkins University Applied Physics Laboratory Staff, "Handbook of Supersonic Aerodynamics, Section 8, Bodies of Revolution," NavWeps Report 1488 (Vol. 3), October 1961.

9. Cooper, Morton and Mayo, Edward E.: Measurements of Local Heat Transfer and Pressure on Six 2-Inch-Diameter Blunt Bodies at a Mach Number of 4.95 and Reynolds Numbers per Foot up to 81×10^6 NASA MEMO 1-3-59L, 1959.

Table 1
Tangent Ogive Aerodynamics
(a) f = 0.5

α	C_m	C_N	C_A	C_L	C_D	L/D
0	0.	0.	1.000	0.	1.000	0.
1.0	-0.009	0.017	1.000	-0.	1.000	-0.
2.0	-0.017	0.035	0.999	-0.	1.000	-0.
3.0	-0.026	0.052	0.999	-0.	1.000	-0.
4.0	-0.035	0.070	0.998	-0.	1.000	-0.
5	-0.044	0.087	0.996	0.	1.000	0.
6.0	-0.052	0.104	0.994	-0.	1.000	-0.
7.0	-0.061	0.121	0.992	-0.	1.000	-0.
8.0	-0.069	0.138	0.990	-0.001	1.000	-0.001
9.0	-0.078	0.156	0.988	-0.001	1.000	-0.001
10	-0.086	0.172	0.985	-0.001	1.000	-0.001
12.5	-0.107	0.214	0.976	-0.002	1.000	-0.002
15	-0.127	0.254	0.966	-0.004	0.999	-0.004
17.5	-0.147	0.294	0.954	-0.007	0.998	-0.007
20	-0.166	0.332	0.941	-0.010	0.997	-0.010
22.5	-0.184	0.368	0.925	-0.014	0.996	-0.014
25	-0.201	0.403	0.908	-0.019	0.994	-0.019
27.5	-0.218	0.436	0.890	-0.025	0.991	-0.025
30	-0.233	0.466	0.870	-0.031	0.987	-0.032
35	-0.261	0.522	0.827	-0.047	0.977	-0.048
40	-0.284	0.568	0.780	-0.066	0.962	-0.069
45	-0.302	0.604	0.728	-0.088	0.942	-0.094
50	-0.315	0.629	0.675	-0.112	0.916	-0.123
55	-0.322	0.644	0.619	-0.137	0.883	-0.156
60	-0.325	0.650	0.562	-0.162	0.844	-0.192
65	-0.322	0.645	0.506	-0.186	0.798	-0.233
70	-0.315	0.631	0.450	-0.207	0.746	-0.278
75	-0.304	0.608	0.396	-0.225	0.690	-0.327
80	-0.289	0.578	0.344	-0.239	0.629	-0.380
85	-0.271	0.542	0.296	-0.247	0.565	-0.437
90	-0.250	0.500	0.250	-0.250	0.500	-0.500
95	-0.227	0.455	0.208	-0.247	0.435	-0.568
100	-0.203	0.407	0.171	-0.239	0.371	-0.644
105	-0.179	0.358	0.137	-0.225	0.310	-0.726
110	-0.155	0.309	0.108	-0.207	0.254	-0.818
115	-0.131	0.262	0.083	-0.186	0.202	-0.922
120	-0.108	0.216	0.062	-0.162	0.156	-1.039
125	-0.087	0.175	0.046	-0.137	0.117	-1.174
130	-0.068	0.137	0.032	-0.112	0.084	-1.333
135	-0.052	0.104	0.021	-0.088	0.058	-1.522
140	-0.038	0.075	0.014	-0.066	0.038	-1.754
145	-0.026	0.052	0.008	-0.047	0.023	-2.047
150	-0.017	0.034	0.004	-0.031	0.013	-2.430
155	-0.010	0.020	0.002	-0.019	0.006	-2.959
160	-0.005	0.010	0.001	-0.010	0.003	-3.742
165	-0.002	0.004	0.	-0.004	0.001	-5.035
170	-0.001	0.001	0.	-0.001	0.	
175	0.	0.	0.	0.	0.	
180	0.	0.	0.	0.	0.	

Table 1 (Continued)
Tangent Ogive Aerodynamics

(b) f = 1

α	C_m	C_N	C_A	C_L	C_D	L/D
0	0.	0.	0.480	0.	0.480	0.
1.0	-0.017	0.026	0.480	0.018	0.481	0.038
2.0	-0.033	0.053	0.480	0.036	0.482	0.075
3.0	-0.050	0.080	0.481	0.054	0.484	0.112
4.0	-0.066	0.106	0.481	0.072	0.488	0.148
5	-0.083	0.132	0.482	0.090	0.492	0.183
6.0	-0.100	0.159	0.483	0.107	0.497	0.216
7.0	-0.116	0.185	0.484	0.125	0.503	0.248
8.0	-0.133	0.211	0.485	0.142	0.510	0.278
9.0	-0.149	0.237	0.487	0.158	0.518	0.305
10	-0.166	0.263	0.488	0.174	0.526	0.331
12.5	-0.207	0.328	0.493	0.213	0.552	0.386
15	-0.248	0.391	0.498	0.249	0.582	0.427
17.5	-0.289	0.453	0.504	0.281	0.617	0.455
20	-0.330	0.514	0.511	0.308	0.656	0.471
22.5	-0.370	0.573	0.517	0.332	0.698	0.476
25	-0.410	0.631	0.525	0.350	0.742	0.472
27.5	-0.449	0.687	0.532	0.364	0.789	0.461
30	-0.487	0.740	0.539	0.372	0.837	0.444
35	-0.561	0.841	0.553	0.372	0.935	0.398
40	-0.629	0.930	0.564	0.350	1.030	0.340
45	-0.691	1.008	0.571	0.309	1.117	0.277
50	-0.745	1.073	0.573	0.251	1.190	0.211
55	-0.791	1.123	0.569	0.178	1.247	0.142
60	-0.825	1.158	0.559	0.094	1.282	0.074
65	-0.848	1.176	0.543	0.005	1.296	0.004
70	-0.860	1.178	0.520	-0.086	1.285	-0.067
75	-0.859	1.163	0.492	-0.174	1.251	-0.139
80	-0.845	1.132	0.458	-0.255	1.194	-0.213
85	-0.820	1.086	0.421	-0.325	1.118	-0.290
90	-0.784	1.026	0.380	-0.380	1.026	-0.371
95	-0.737	0.954	0.337	-0.419	0.921	-0.455
100	-0.683	0.872	0.293	-0.440	0.808	-0.545
105	-0.621	0.783	0.249	-0.444	0.692	-0.641
110	-0.554	0.690	0.207	-0.430	0.577	-0.746
115	-0.484	0.594	0.167	-0.402	0.468	-0.860
120	-0.413	0.500	0.131	-0.363	0.367	-0.988
125	-0.343	0.409	0.098	-0.315	0.278	-1.132
130	-0.277	0.324	0.071	-0.263	0.203	-1.297
135	-0.215	0.248	0.049	-0.210	0.141	-1.493
140	-0.161	0.182	0.032	-0.160	0.092	-1.729
145	-0.113	0.126	0.019	-0.115	0.057	-2.026
150	-0.075	0.082	0.011	-0.077	0.032	-2.413
155	-0.045	0.049	0.005	-0.047	0.016	-2.945
160	-0.024	0.026	0.002	-0.025	0.007	-3.732
165	-0.011	0.011	0.001	-0.011	0.002	-5.027
170	-0.003	0.003	0.	-0.003	0.	
175	0.	0.	0.	0.	0.	
180	0.	0.	0.	0.	0.	

Table 1 (Continued)
Tangent Ogive Aerodynamics
(c) f = 2

α	C_m	C_N	C_A	C_L	C_D	L/D
0	0.	0.	0.152	0.	0.152	0.
1.0	-0.033	0.032	0.152	0.030	0.153	0.193
2.0	-0.066	0.064	0.153	0.059	0.155	0.381
3.0	-0.099	0.097	0.154	0.089	0.159	0.557
4.0	-0.132	0.129	0.156	0.118	0.165	0.717
5	-0.166	0.162	0.158	0.147	0.172	0.859
6.0	-0.200	0.194	0.161	0.177	0.180	0.981
7.0	-0.234	0.227	0.164	0.206	0.190	1.082
8.0	-0.269	0.260	0.167	0.235	0.202	1.164
9.0	-0.305	0.294	0.171	0.263	0.215	1.227
10	-0.341	0.327	0.175	0.292	0.229	1.273
12.5	-0.436	0.412	0.187	0.362	0.272	1.330
15	-0.534	0.499	0.202	0.429	0.324	1.326
17.5	-0.638	0.587	0.218	0.495	0.384	1.287
20	-0.747	0.678	0.235	0.557	0.453	1.229
22.5	-0.861	0.771	0.254	0.615	0.530	1.161
25	-0.980	0.866	0.274	0.669	0.614	1.090
27.5	-1.101	0.962	0.294	0.718	0.705	1.018
30	-1.226	1.060	0.314	0.761	0.802	0.949
35	-1.481	1.256	0.354	0.826	1.010	0.818
40	-1.737	1.449	0.392	0.858	1.231	0.697
45	-1.986	1.633	0.426	0.853	1.456	0.586
50	-2.220	1.803	0.457	0.809	1.674	0.483
55	-2.433	1.953	0.481	0.726	1.876	0.387
60	-2.618	2.080	0.500	0.607	2.051	0.296
65	-2.770	2.179	0.512	0.457	2.191	0.209
70	-2.883	2.248	0.516	0.284	2.289	0.124
75	-2.955	2.283	0.513	0.095	2.338	0.041
80	-2.984	2.285	0.503	-0.099	2.338	-0.042
85	-2.967	2.253	0.486	-0.288	2.287	-0.126
90	-2.907	2.189	0.462	-0.462	2.189	-0.211
95	-2.804	2.093	0.432	-0.613	2.047	-0.299
100	-2.663	1.969	0.397	-0.733	1.870	-0.392
105	-2.486	1.821	0.359	-0.818	1.666	-0.491
110	-2.280	1.654	0.317	-0.864	1.446	-0.598
115	-2.051	1.471	0.274	-0.870	1.218	-0.715
120	-1.806	1.280	0.231	-0.840	0.993	-0.846
125	-1.551	1.085	0.189	-0.777	0.781	-0.995
130	-1.296	0.893	0.148	-0.688	0.588	-1.168
135	-1.048	0.709	0.112	-0.580	0.422	-1.374
140	-0.813	0.539	0.079	-0.464	0.285	-1.625
145	-0.600	0.388	0.052	-0.348	0.179	-1.938
150	-0.414	0.260	0.031	-0.240	0.103	-2.342
155	-0.261	0.158	0.016	-0.150	0.052	-2.890
160	-0.144	0.084	0.007	-0.082	0.022	-3.690
165	-0.065	0.037	0.002	-0.036	0.007	-4.997
170	-0.021	0.011	0.001	-0.011	0.001	-7.576
175	-0.003	0.001	0.	-0.001	0.	
180	0.	0.	0.	0.	0.	

Table 1 (Continued)
Tangent Ogive Aerodynamics
(d) f = 3

α	C_m	C_N	C_A	C_L	C_D	L/D
0	0.	0.	0.071	0.	0.071	0.
1.0	-0.049	0.034	0.071	0.032	0.072	0.451
2.0	-0.098	0.068	0.072	0.065	0.074	0.871
3.0	-0.149	0.102	0.074	0.098	0.079	1.238
4.0	-0.200	0.136	0.075	0.130	0.085	1.537
5	-0.252	0.171	0.078	0.163	0.092	1.765
6.0	-0.306	0.206	0.081	0.196	0.102	1.928
7.0	-0.362	0.242	0.084	0.230	0.113	2.033
8.0	-0.420	0.278	0.088	0.263	0.126	2.092
9.0	-0.481	0.316	0.092	0.297	0.141	2.115
10	-0.543	0.354	0.097	0.332	0.157	2.112
12.5	-0.711	0.453	0.111	0.419	0.206	2.032
15	-0.896	0.560	0.126	0.508	0.267	1.905
17.5	-1.097	0.673	0.143	0.599	0.339	1.766
20	-1.315	0.794	0.162	0.690	0.424	1.630
22.5	-1.546	0.921	0.181	0.781	0.520	1.503
25	-1.791	1.054	0.202	0.870	0.628	1.385
27.5	-2.048	1.192	0.222	0.954	0.747	1.277
30	-2.313	1.333	0.243	1.033	0.878	1.177
35	-2.864	1.625	0.286	1.167	1.166	1.001
40	-3.428	1.919	0.328	1.259	1.485	0.848
45	-3.987	2.207	0.368	1.300	1.821	0.714
50	-4.525	2.481	0.405	1.284	2.161	0.594
55	-5.025	2.731	0.438	1.208	2.488	0.486
60	-5.472	2.951	0.465	1.073	2.788	0.385
65	-5.853	3.134	0.486	0.884	3.045	0.290
70	-6.156	3.274	0.500	0.650	3.247	0.200
75	-6.372	3.366	0.506	0.382	3.383	0.113
80	-6.493	3.409	0.506	0.094	3.445	0.027
85	-6.518	3.401	0.498	-0.199	3.431	-0.058
90	-6.444	3.342	0.482	-0.482	3.342	-0.144
95	-6.274	3.234	0.460	-0.740	3.181	-0.233
100	-6.013	3.079	0.432	-0.960	2.958	-0.324
105	-5.670	2.884	0.398	-1.131	2.683	-0.422
110	-5.254	2.654	0.360	-1.246	2.370	-0.526
115	-4.778	2.395	0.319	-1.302	2.036	-0.639
120	-4.257	2.116	0.276	-1.297	1.694	-0.766
125	-3.706	1.825	0.233	-1.238	1.361	-0.909
130	-3.143	1.531	0.190	-1.130	1.050	-1.076
135	-2.584	1.243	0.150	-0.984	0.773	-1.274
140	-2.046	0.969	0.112	-0.814	0.537	-1.516
145	-1.546	0.718	0.079	-0.634	0.347	-1.824
150	-1.098	0.498	0.051	-0.457	0.205	-2.230
155	-0.717	0.315	0.029	-0.298	0.107	-2.792
160	-0.413	0.174	0.014	-0.168	0.046	-3.615
165	-0.194	0.078	0.005	-0.076	0.015	-4.944
170	-0.064	0.024	0.001	-0.024	0.003	-7.542
175	-0.009	0.003	0.	-0.003	0.	
180	0.	0.	0.	0.	0.	

Table 1 (Continued)
Tangent Ogive Aerodynamics
(e) f = 4

α	C_m	C_N	C_A	C_L	C_D	L/D
0	0.	0.	0.041	0.	0.041	0.
1.0	-0.065	0.034	0.041	0.034	0.042	0.806
2.0	-0.132	0.069	0.042	0.067	0.044	1.519
3.0	-0.200	0.104	0.043	0.101	0.049	2.080
4.0	-0.270	0.139	0.045	0.136	0.055	2.473
5	-0.344	0.175	0.048	0.171	0.063	2.715
6.0	-0.422	0.213	0.051	0.206	0.073	2.839
7.0	-0.504	0.252	0.054	0.243	0.084	2.877
8.0	-0.591	0.292	0.058	0.281	0.098	2.858
9.0	-0.682	0.333	0.062	0.319	0.114	2.803
10	-0.779	0.376	0.067	0.359	0.132	2.726
12.5	-1.046	0.492	0.081	0.463	0.185	2.499
15	-1.347	0.620	0.096	0.574	0.253	2.268
17.5	-1.680	0.760	0.112	0.691	0.336	2.058
20	-2.045	0.912	0.130	0.812	0.434	1.870
22.5	-2.437	1.073	0.149	0.934	0.548	1.703
25	-2.855	1.244	0.169	1.056	0.679	1.555
27.5	-3.295	1.422	0.189	1.174	0.825	1.424
30	-3.753	1.607	0.210	1.287	0.986	1.305
35	-4.712	1.991	0.253	1.486	1.350	1.101
40	-5.703	2.384	0.296	1.636	1.760	0.930
45	-6.696	2.774	0.338	1.722	2.201	0.783
50	-7.660	3.149	0.378	1.735	2.655	0.653
55	-8.566	3.498	0.413	1.668	3.102	0.538
60	-9.388	3.809	0.444	1.520	3.521	0.432
65	-10.099	4.075	0.470	1.297	3.891	0.333
70	-10.678	4.286	0.488	1.007	4.194	0.240
75	-11.108	4.436	0.500	0.665	4.414	0.151
80	-11.375	4.521	0.504	0.289	4.540	0.064
85	-11.472	4.538	0.501	-0.103	4.564	-0.023
90	-11.395	4.486	0.490	-0.490	4.486	-0.109
95	-11.148	4.367	0.472	-0.851	4.310	-0.197
100	-10.736	4.186	0.447	-1.167	4.044	-0.289
105	-10.173	3.946	0.417	-1.424	3.704	-0.384
110	-9.477	3.656	0.382	-1.609	3.305	-0.487
115	-8.667	3.324	0.342	-1.715	2.868	-0.598
120	-7.769	2.961	0.301	-1.741	2.414	-0.721
125	-6.810	2.577	0.257	-1.689	1.963	-0.860
130	-5.819	2.184	0.214	-1.568	1.536	-1.021
135	-4.827	1.794	0.172	-1.390	1.147	-1.212
140	-3.862	1.420	0.132	-1.172	0.811	-1.445
145	-2.956	1.071	0.096	-0.932	0.535	-1.742
150	-2.134	0.759	0.065	-0.690	0.323	-2.134
155	-1.423	0.493	0.039	-0.464	0.173	-2.684
160	-0.843	0.282	0.020	-0.272	0.077	-3.510
165	-0.412	0.130	0.008	-0.128	0.026	-4.867
170	-0.140	0.041	0.002	-0.041	0.005	-7.495
175	-0.020	0.005	0.	-0.005	0.	
180	0.	0.	0.	0.	0.	

Table 1 (Continued
Tangent Ogive Aerodynamics
(f) f = 5

α	C_m	C_N	C_A	C_L	C_D	L/D
0	0.	0.	0.026	0.	0.026	0.
1.0	-0.082	0.034	0.027	0.034	0.027	1.253
2.0	-0.166	0.069	0.027	0.068	0.030	2.291
3.0	-0.253	0.105	0.029	0.103	0.034	3.009
4.0	-0.345	0.142	0.031	0.139	0.041	3.420
5	-0.443	0.180	0.033	0.176	0.049	3.598
6.0	-0.548	0.219	0.036	0.214	0.059	3.624
7.0	-0.661	0.261	0.040	0.254	0.071	3.560
8.0	-0.783	0.305	0.044	0.296	0.086	3.448
9.0	-0.914	0.351	0.048	0.339	0.102	3.313
10	-1.054	0.400	0.053	0.385	0.121	3.171
12.5	-1.444	0.534	0.066	0.507	0.180	2.823
15	-1.891	0.685	0.080	0.641	0.255	2.516
17.5	-2.390	0.852	0.096	0.783	0.348	2.253
20	-2.940	1.034	0.113	0.933	0.460	2.028
22.5	-3.535	1.229	0.132	1.085	0.592	1.834
25	-4.171	1.437	0.151	1.239	0.744	1.665
27.5	-4.843	1.656	0.171	1.390	0.916	1.517
30	-5.547	1.884	0.192	1.536	1.108	1.386
35	-7.026	2.359	0.234	1.798	1.545	1.164
40	-8.563	2.849	0.278	2.004	2.044	0.980
45	-10.112	3.340	0.320	2.135	2.588	0.825
50	-11.625	3.815	0.361	2.176	3.154	0.690
55	-13.057	4.261	0.398	2.117	3.718	0.569
60	-14.364	4.663	0.431	1.958	4.254	0.460
65	-15.506	5.011	0.459	1.702	4.735	0.359
70	-16.449	5.292	0.480	1.359	5.138	0.264
75	-17.164	5.500	0.495	0.946	5.441	0.174
80	-17.629	5.627	0.502	0.483	5.628	0.086
85	-17.831	5.669	0.501	-0.005	5.691	-0.001
90	-17.762	5.626	0.493	-0.493	5.626	-0.088
95	-17.425	5.498	0.478	-0.956	5.435	-0.176
100	-16.831	5.289	0.456	-1.368	5.130	-0.267
105	-15.997	5.006	0.428	-1.709	4.725	-0.362
110	-14.948	4.658	0.394	-1.964	4.242	-0.463
115	-13.718	4.255	0.356	-2.121	3.706	-0.572
120	-12.342	3.809	0.315	-2.177	3.141	-0.693
125	-10.863	3.333	0.272	-2.135	2.574	-0.829
130	-9.326	2.843	0.229	-2.003	2.031	-0.986
135	-7.777	2.353	0.186	-1.795	1.532	-1.172
140	-6.263	1.878	0.146	-1.532	1.095	-1.398
145	-4.831	1.432	0.108	-1.235	0.733	-1.685
150	-3.524	1.029	0.075	-0.928	0.450	-2.065
155	-2.382	0.681	0.047	-0.637	0.245	-2.598
160	-1.439	0.399	0.025	-0.384	0.113	-3.407
165	-0.723	0.191	0.011	-0.187	0.039	-4.766
170	-0.255	0.062	0.003	-0.062	0.008	-7.431
175	-0.037	0.008	0.	-0.008	0.001	-15.178
180	0.	0.	0.	0.	0.	

Table 1 (Continued
Tangent Ogive Aerodynamics

(g) f = 6

α	C_m	C_N	C_A	C_L	C_D	L/D
0	0.	0.	0.018	0.	0.018	0.
1.0	-0.098	0.035	0.019	0.034	0.019	1.786
2.0	-0.200	0.070	0.020	0.069	0.022	3.153
3.0	-0.307	0.106	0.021	0.105	0.026	3.961
4.0	-0.423	0.144	0.023	0.142	0.033	4.311
5	-0.549	0.184	0.026	0.181	0.041	4.371
6.0	-0.686	0.226	0.028	0.222	0.052	4.273
7.0	-0.837	0.271	0.032	0.265	0.065	4.102
8.0	-1.001	0.319	0.036	0.311	0.080	3.903
9.0	-1.178	0.371	0.040	0.360	0.097	3.700
10	-1.370	0.426	0.044	0.412	0.118	3.504
12.5	-1.908	0.578	0.057	0.552	0.180	3.062
15	-2.529	0.752	0.071	0.708	0.263	2.695
17.5	-3.228	0.946	0.086	0.876	0.366	2.392
20	-4.000	1.159	0.103	1.054	0.493	2.139
22.5	-4.839	1.388	0.120	1.236	0.642	1.924
25	-5.739	1.633	0.139	1.421	0.816	1.741
27.5	-6.693	1.892	0.159	1.604	1.014	1.582
30	-7.694	2.162	0.180	1.782	1.236	1.442
35	-9.805	2.728	0.222	2.107	1.746	1.207
40	-12.008	3.315	0.265	2.369	2.334	1.015
45	-14.236	3.905	0.308	2.543	2.979	0.854
50	-16.421	4.480	0.350	2.612	3.656	0.714
55	-18.498	5.022	0.388	2.562	4.336	0.591
60	-20.402	5.515	0.422	2.392	4.987	0.480
65	-22.076	5.944	0.451	2.103	5.578	0.377
70	-23.470	6.297	0.474	1.708	6.079	0.281
75	-24.541	6.561	0.491	1.224	6.465	0.189
80	-25.255	6.730	0.500	0.676	6.714	0.101
85	-25.593	6.798	0.501	0.093	6.816	0.014
90	-25.543	6.763	0.495	-0.495	6.763	-0.073
95	-25.106	6.626	0.482	-1.058	6.559	-0.161
100	-24.297	6.391	0.462	-1.564	6.214	-0.252
105	-23.140	6.066	0.435	-1.990	5.746	-0.346
110	-21.669	5.660	0.403	-2.314	5.181	-0.447
115	-19.930	5.185	0.366	-2.523	4.545	-0.555
120	-17.976	4.657	0.325	-2.610	3.870	-0.674
125	-15.865	4.091	0.283	-2.578	3.189	-0.808
130	-13.662	3.504	0.239	-2.436	2.530	-0.963
135	-11.434	2.914	0.196	-2.199	1.922	-1.144
140	-9.249	2.339	0.155	-1.891	1.385	-1.366
145	-7.172	1.797	0.116	-1.539	0.935	-1.645
150	-5.268	1.304	0.082	-1.170	0.581	-2.014
155	-3.593	0.874	0.053	-0.814	0.322	-2.532
160	-2.199	0.522	0.030	-0.500	0.151	-3.320
165	-1.128	0.257	0.013	-0.251	0.054	-4.661
170	-0.412	0.087	0.003	-0.086	0.012	-7.351
175	-0.062	0.012	0.	-0.012	0.001	-15.142
180	0.	0.	0.	0.	0.	

Table 1 (Continued)
Tangent Ogive Aerodynamics
(h) f = 7

α	C_m	C_N	C_A	C_L	C_D	L/D
0	0.	0.	0.014	0.	0.014	0.
1.0	-0.115	0.035	0.014	0.034	0.014	2.398
2.0	-0.235	0.070	0.015	0.070	0.017	4.073
3.0	-0.364	0.107	0.016	0.106	0.022	4.892
4.0	-0.506	0.146	0.018	0.145	0.028	5.117
5	-0.664	0.188	0.021	0.186	0.037	5.029
6.0	-0.838	0.233	0.024	0.230	0.048	4.805
7.0	-1.032	0.282	0.027	0.277	0.061	4.536
8.0	-1.245	0.335	0.031	0.328	0.077	4.263
9.0	-1.476	0.392	0.034	0.382	0.095	4.003
10	-1.728	0.454	0.039	0.440	0.117	3.762
12.5	-2.438	0.625	0.051	0.599	0.185	3.244
15	-3.262	0.822	0.064	0.777	0.275	2.830
17.5	-4.194	1.042	0.079	0.970	0.389	2.496
20	-5.226	1.285	0.095	1.175	0.529	2.221
22.5	-6.351	1.549	0.113	1.388	0.697	1.991
25	-7.561	1.831	0.131	1.604	0.893	1.796
27.5	-8.845	2.129	0.151	1.818	1.117	1.628
30	-10.195	2.441	0.171	2.028	1.368	1.482
35	-13.049	3.097	0.213	2.415	1.951	1.238
40	-16.037	3.781	0.257	2.731	2.627	1.040
45	-19.067	4.470	0.300	2.949	3.373	0.874
50	-22.047	5.144	0.342	3.045	4.160	0.732
55	-24.887	5.782	0.381	3.005	4.955	0.606
60	-27.501	6.366	0.416	2.823	5.721	0.493
65	-29.808	6.877	0.446	2.502	6.421	0.390
70	-31.740	7.299	0.470	2.055	7.020	0.293
75	-33.237	7.621	0.488	1.501	7.487	0.200
80	-34.254	7.832	0.498	0.869	7.799	0.111
85	-34.759	7.925	0.501	0.191	7.938	0.024
90	-34.738	7.898	0.497	-0.497	7.898	-0.063
95	-34.192	7.752	0.485	-1.158	7.681	-0.151
100	-33.136	7.492	0.465	-1.759	7.297	-0.241
105	-31.603	7.124	0.440	-2.269	6.768	-0.335
110	-29.639	6.661	0.408	-2.662	6.120	-0.435
115	-27.305	6.116	0.372	-2.922	5.386	-0.543
120	-24.671	5.506	0.332	-3.041	4.602	-0.661
125	-21.816	4.849	0.290	-3.019	3.806	-0.793
130	-18.829	4.166	0.247	-2.867	3.032	-0.945
135	-15.799	3.477	0.204	-2.602	2.314	-1.124
140	-12.818	2.803	0.162	-2.251	1.678	-1.342
145	-9.978	2.164	0.123	-1.843	1.141	-1.615
150	-7.365	1.581	0.087	-1.412	0.715	-1.977
155	-5.057	1.070	0.057	-0.994	0.400	-2.482
160	-3.125	0.647	0.033	-0.619	0.190	-3.251
165	-1.628	0.325	0.015	-0.318	0.070	-4.565
170	-0.610	0.114	0.004	-0.113	0.016	-7.254
175	-0.096	0.016	0.	-0.016	0.001	-15.098
180	0.	0.	0.	0.	0.	

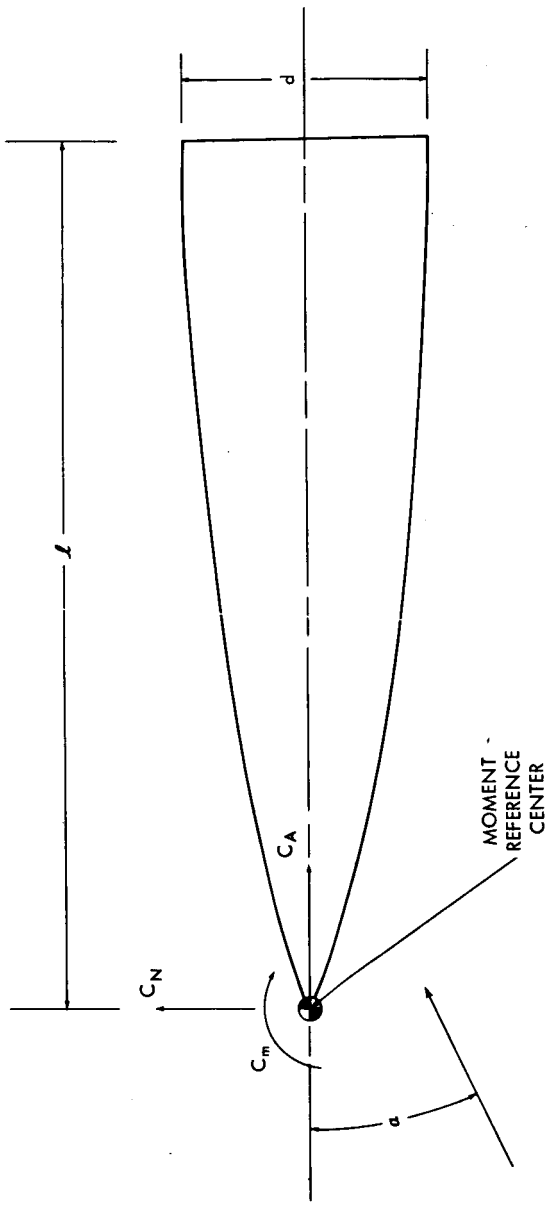

RANGE OF VARIABLES:

$0.5 \leq \frac{\ell}{d} \leq 7$

$0 \leq \alpha \leq 180$

Figure 1–Aerodynamic reference system.

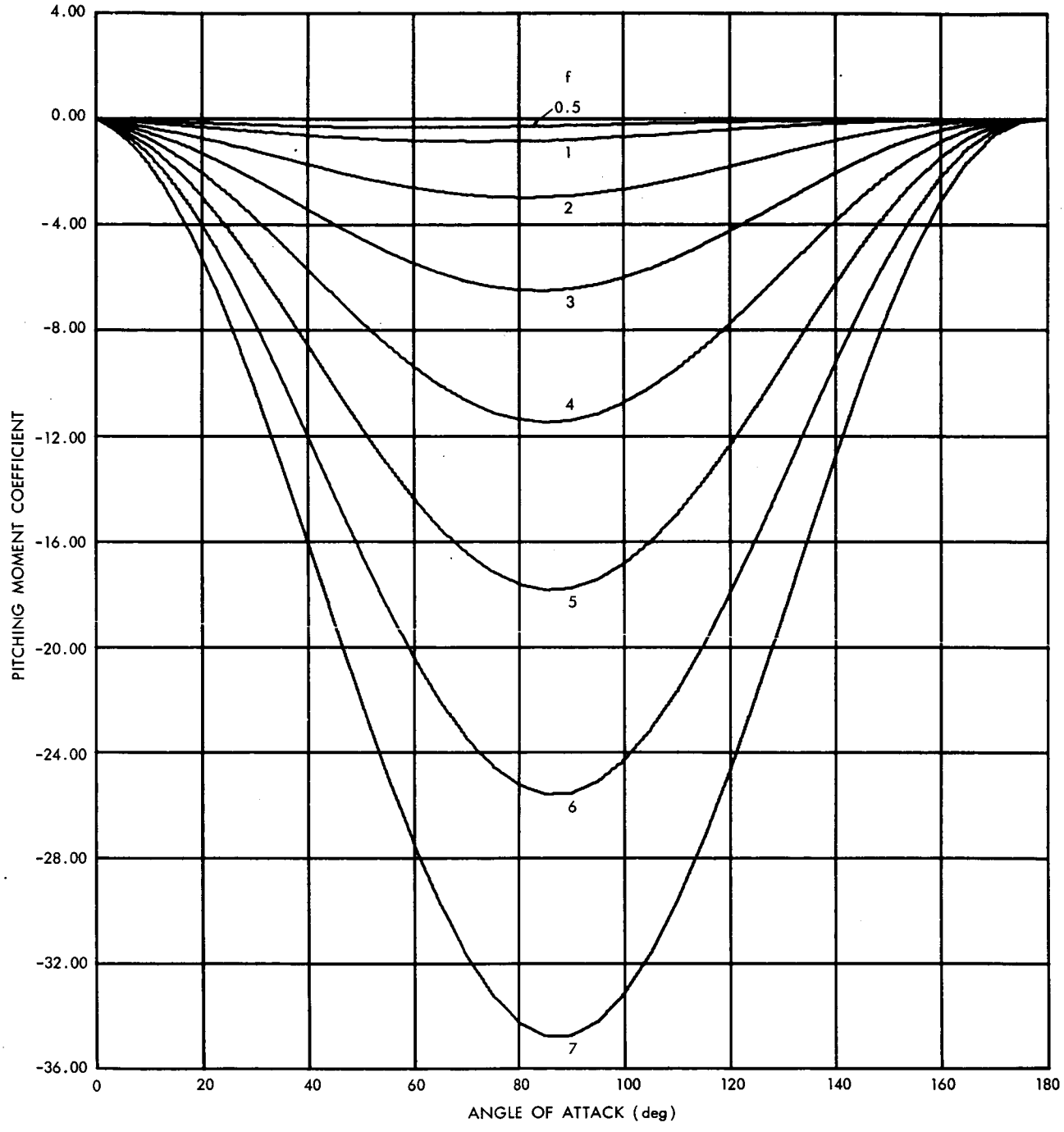

(a) Pitching Moment Characteristics

Figure 2–Tangent ogive aerodynamics.

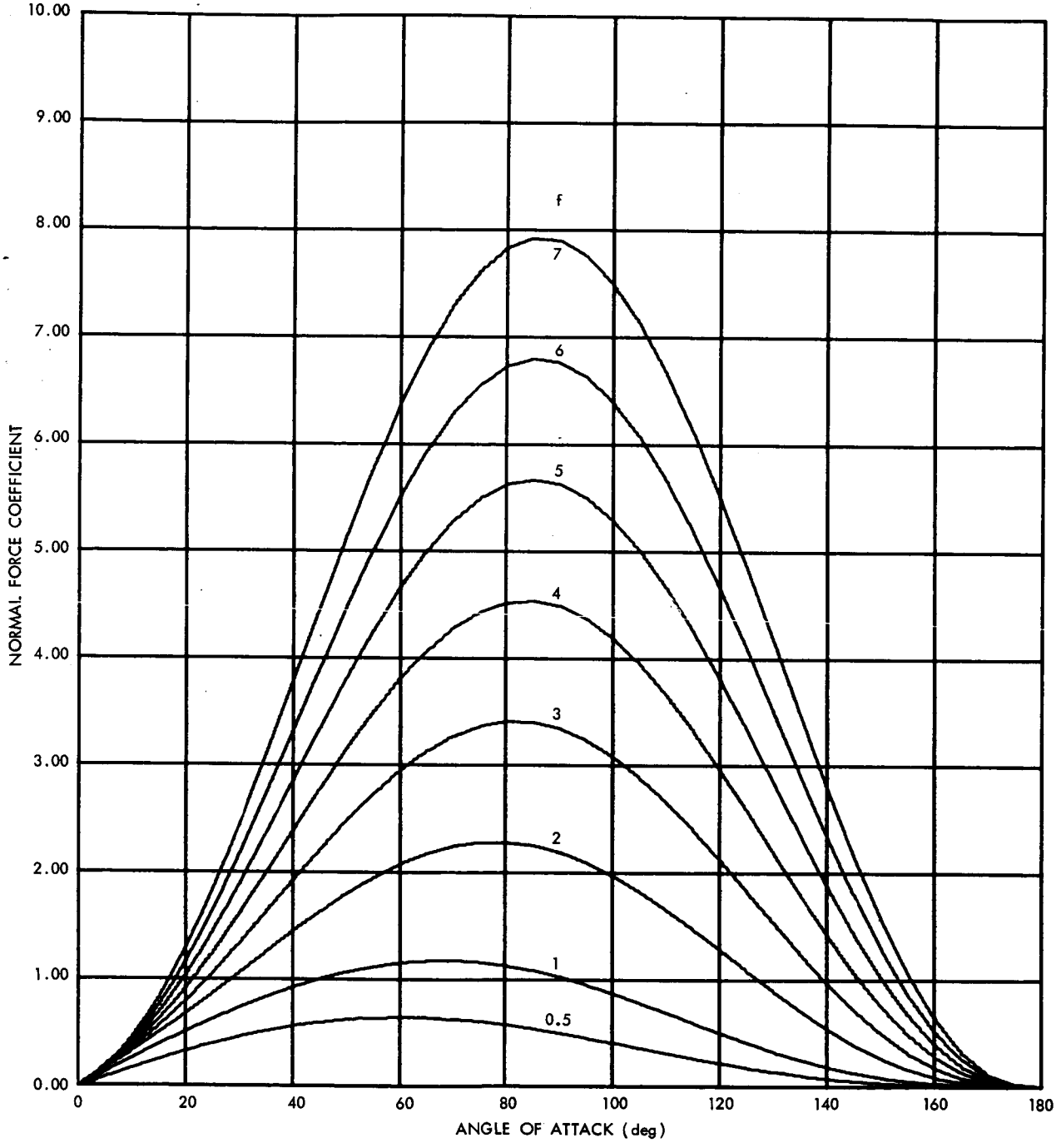

(b) Normal Force Characteristics

Figure 2–Tangent ogive aerodynamics.

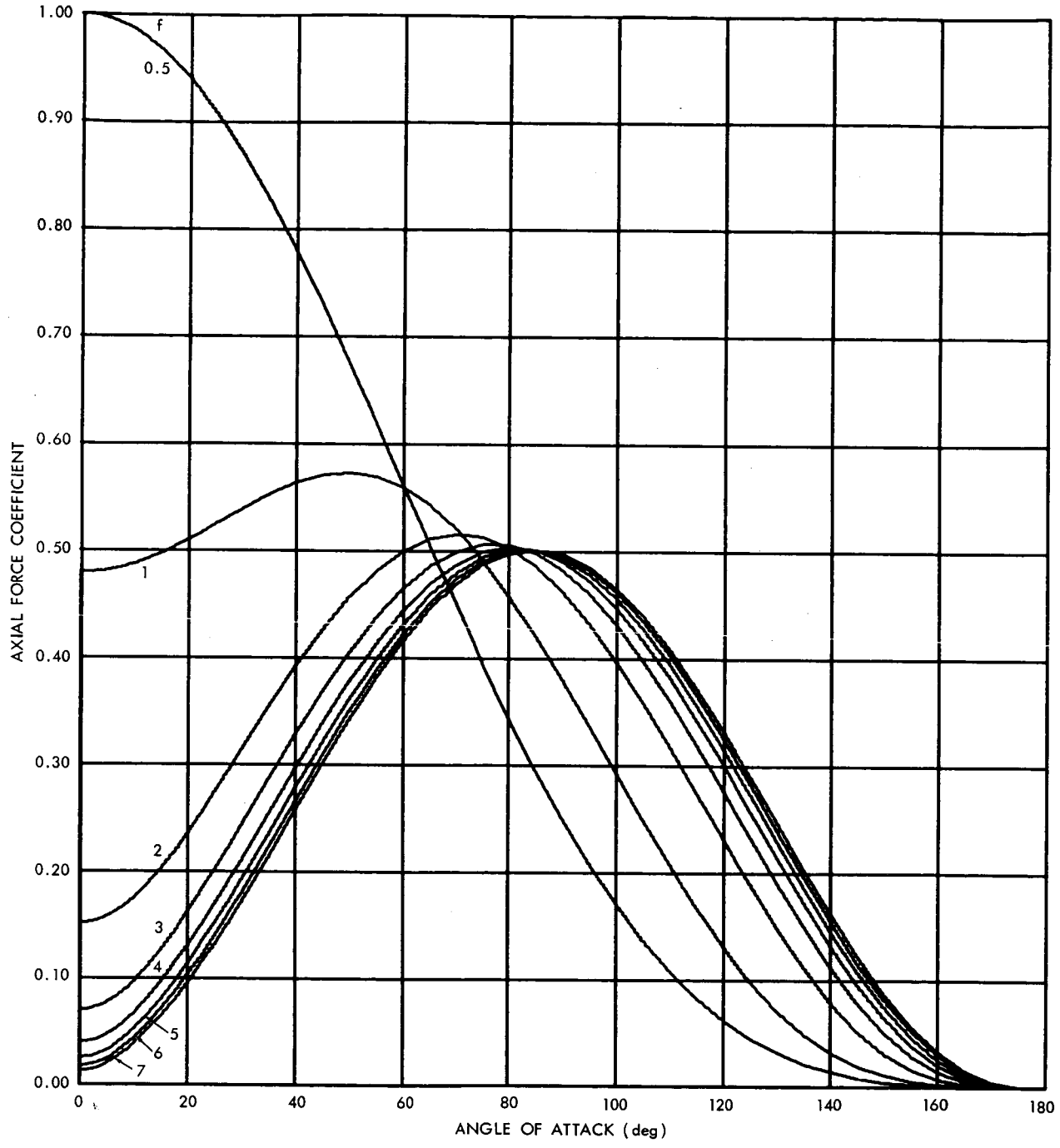

(c) Axial Force Characteristics

Figure 2–Tangent ogive aerodynamics.

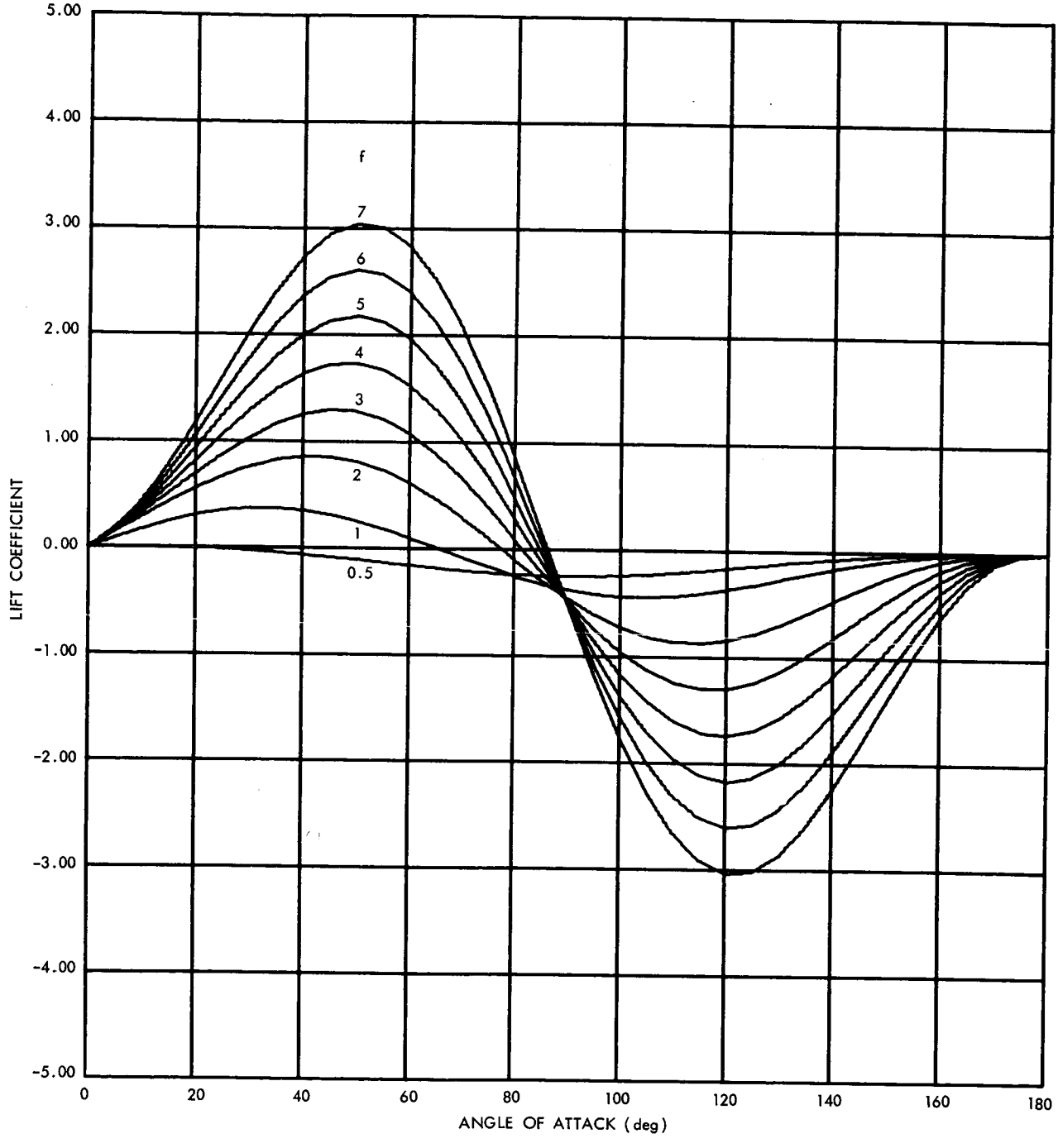

(d) Lift Force Characteristics

Figure 2–Tangent ogive aerodynamics.

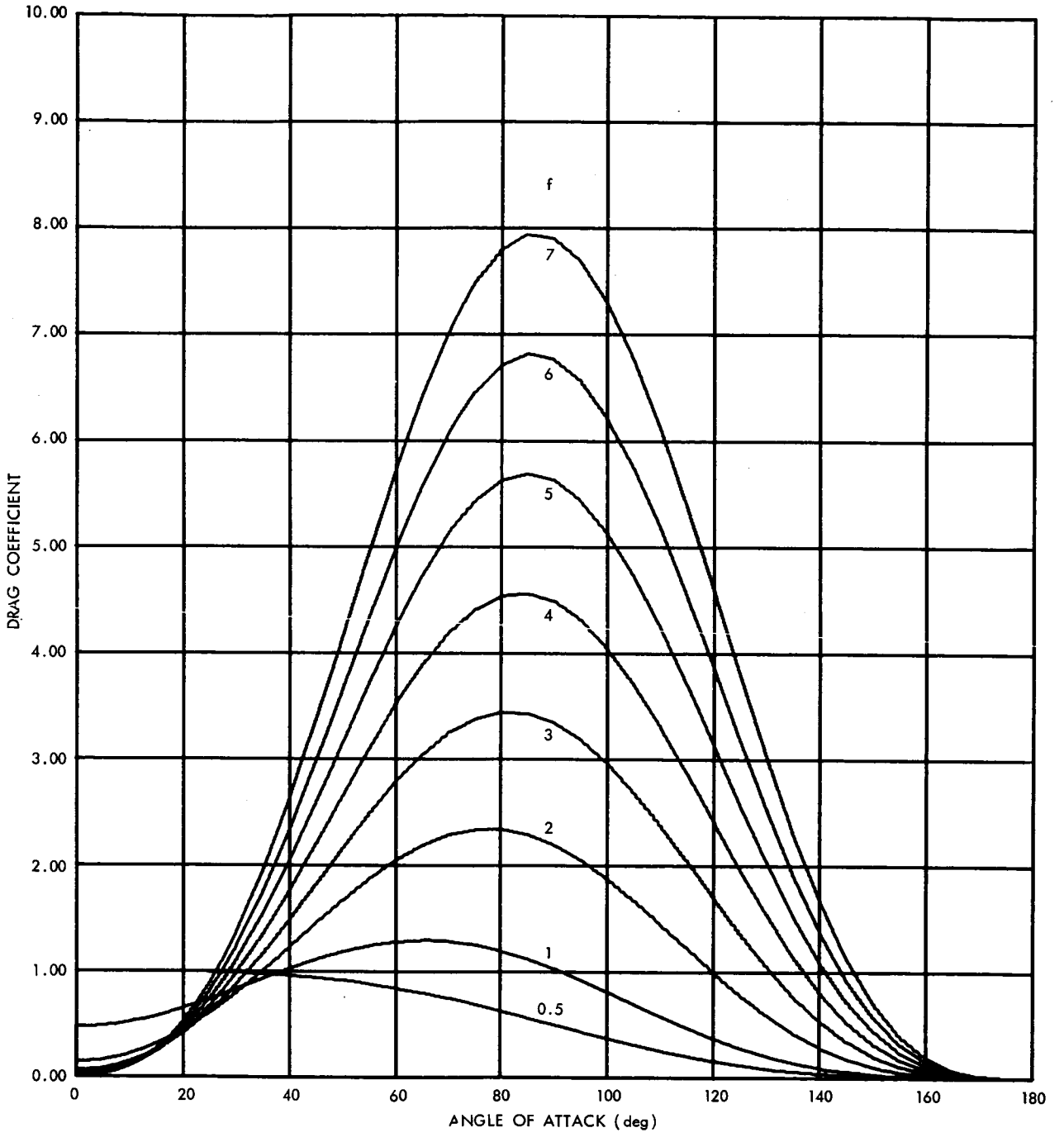

(e) Drag Force Characteristics

Figure 2–Tangent ogive aerodynamics.

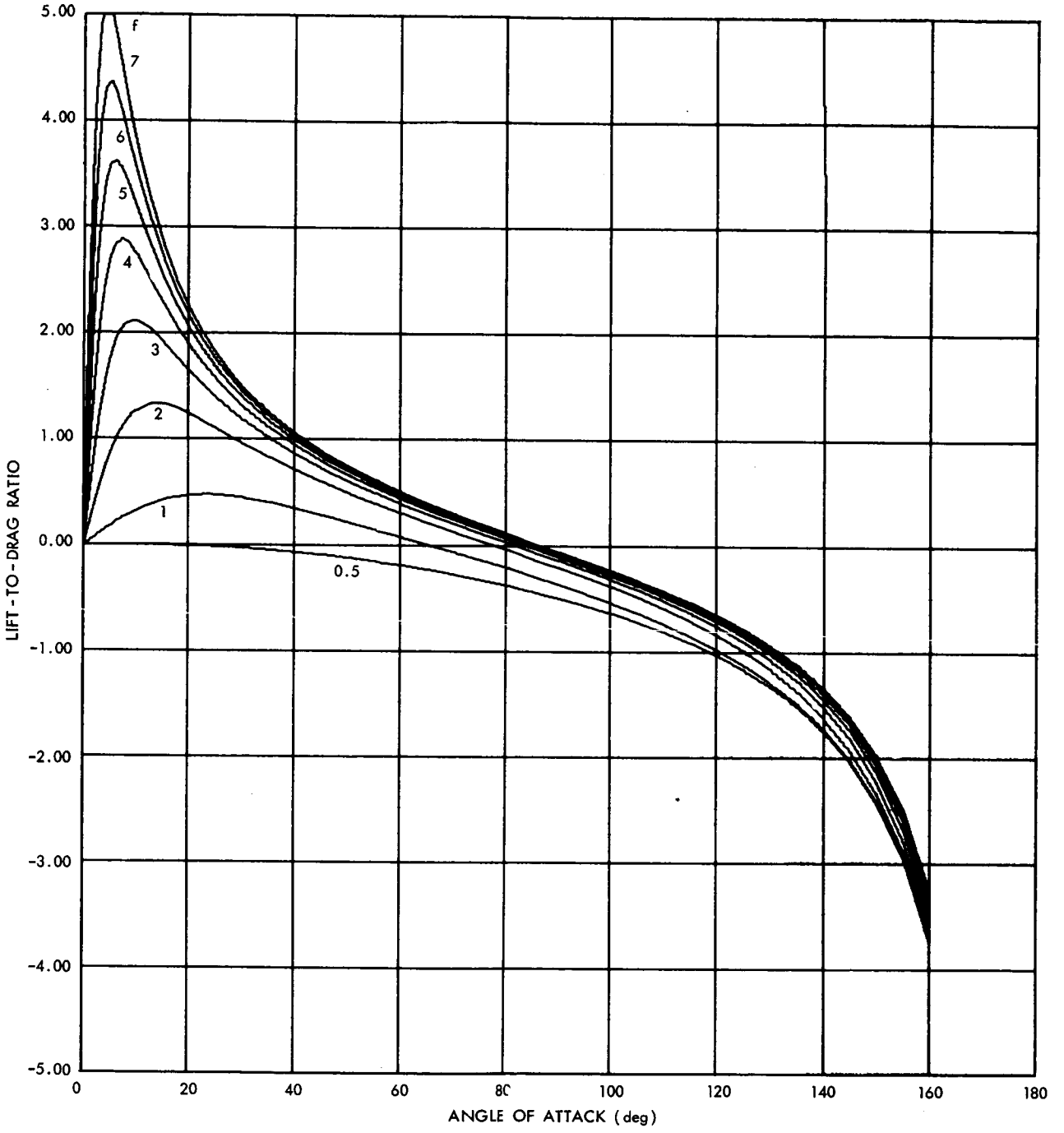

(f) Lift-to-Drag Ratio

Figure 2–Tangent ogive aerodynamics.

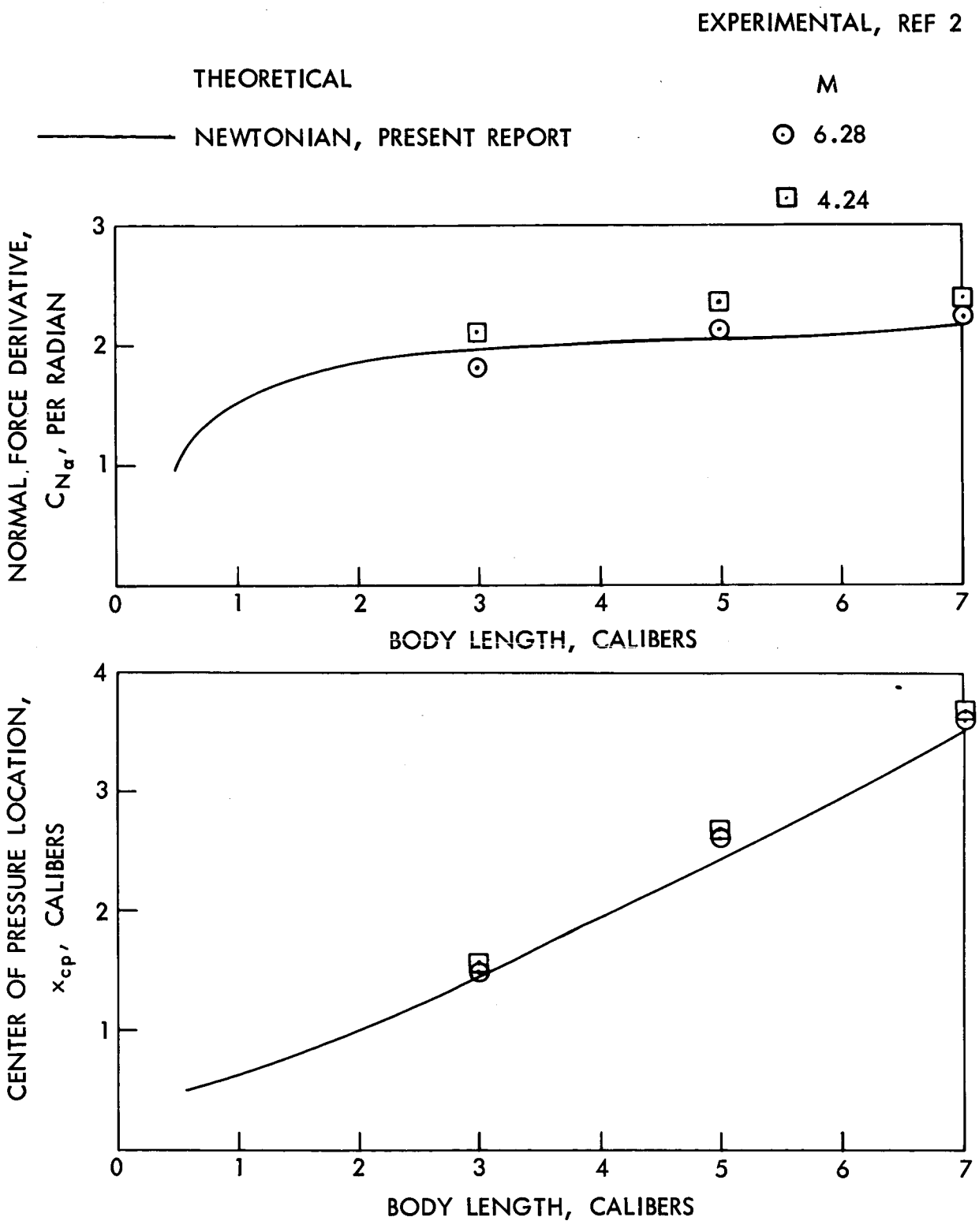

Figure 3–Tangent ogive near zero lift stability characteristics.

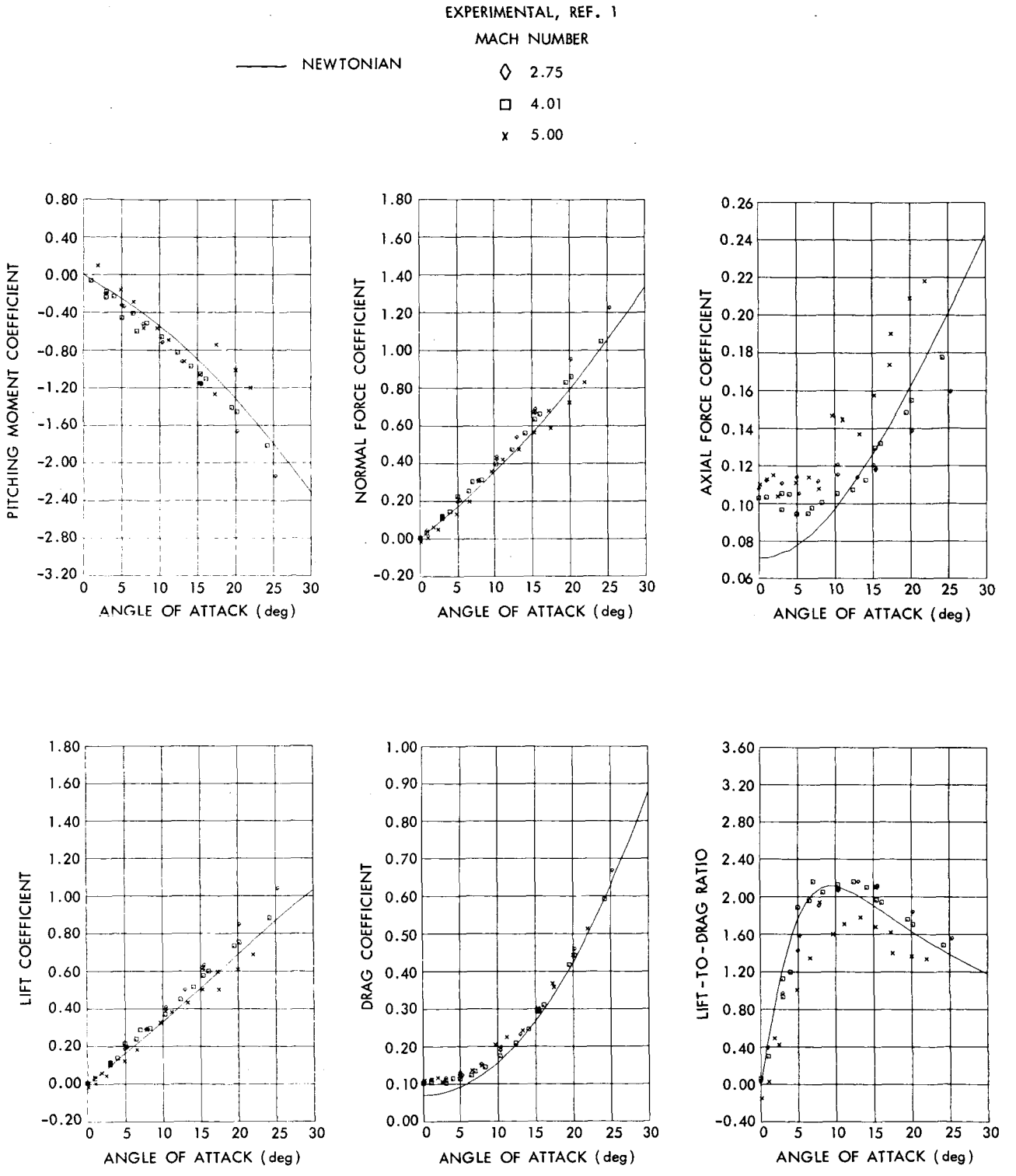

(a) f = 3

Figure 4–Comparison of theoretical and experimental aerodynamic characteristics of fineness ratio 3, 5 and 7 tangent ogive bodies.

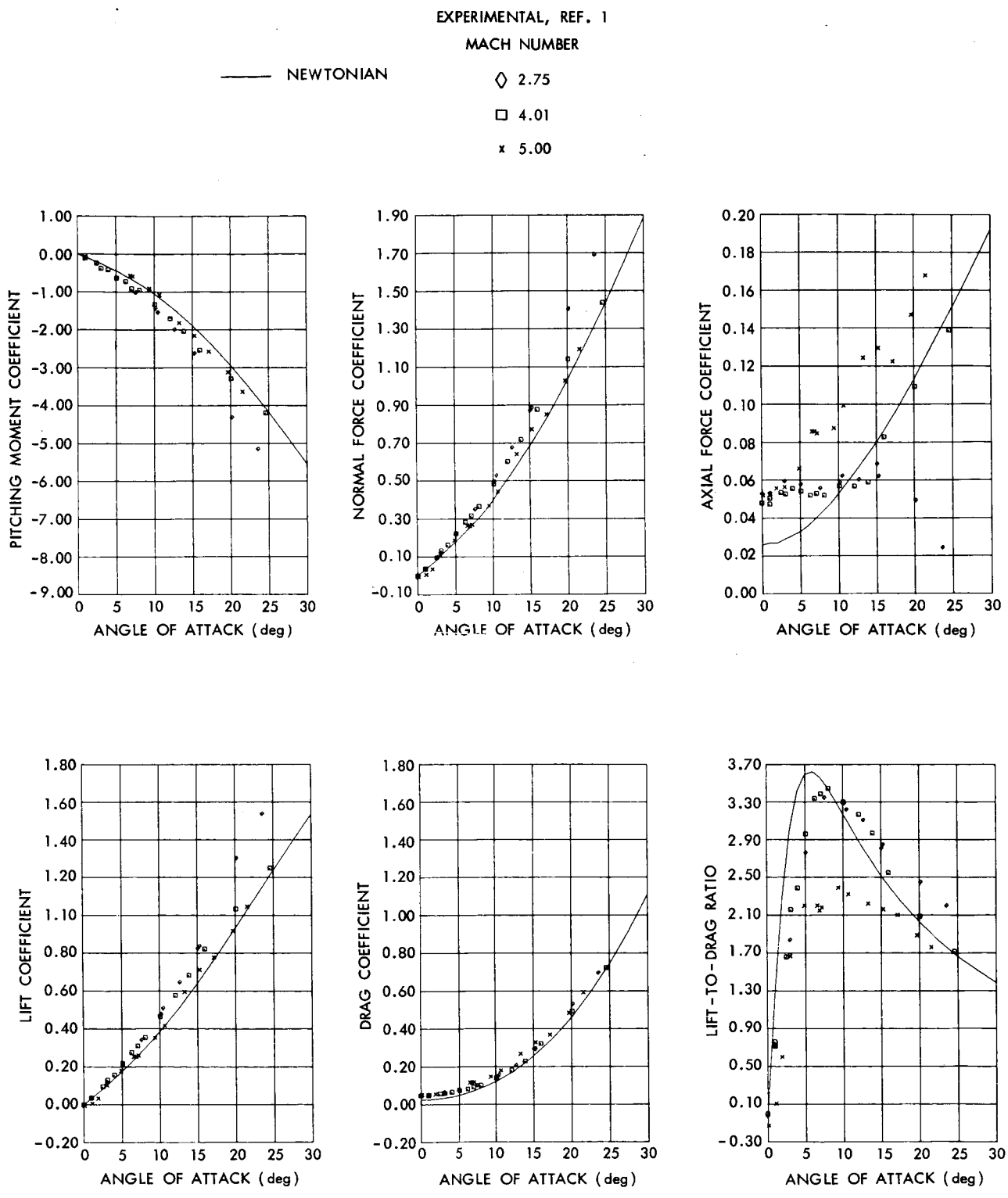

(b) f = 5

Figure 4–Comparison of theoretical and experimental aerodynamic characteristics of fineness ratio 3, 5 and 7 tangent ogive bodies.

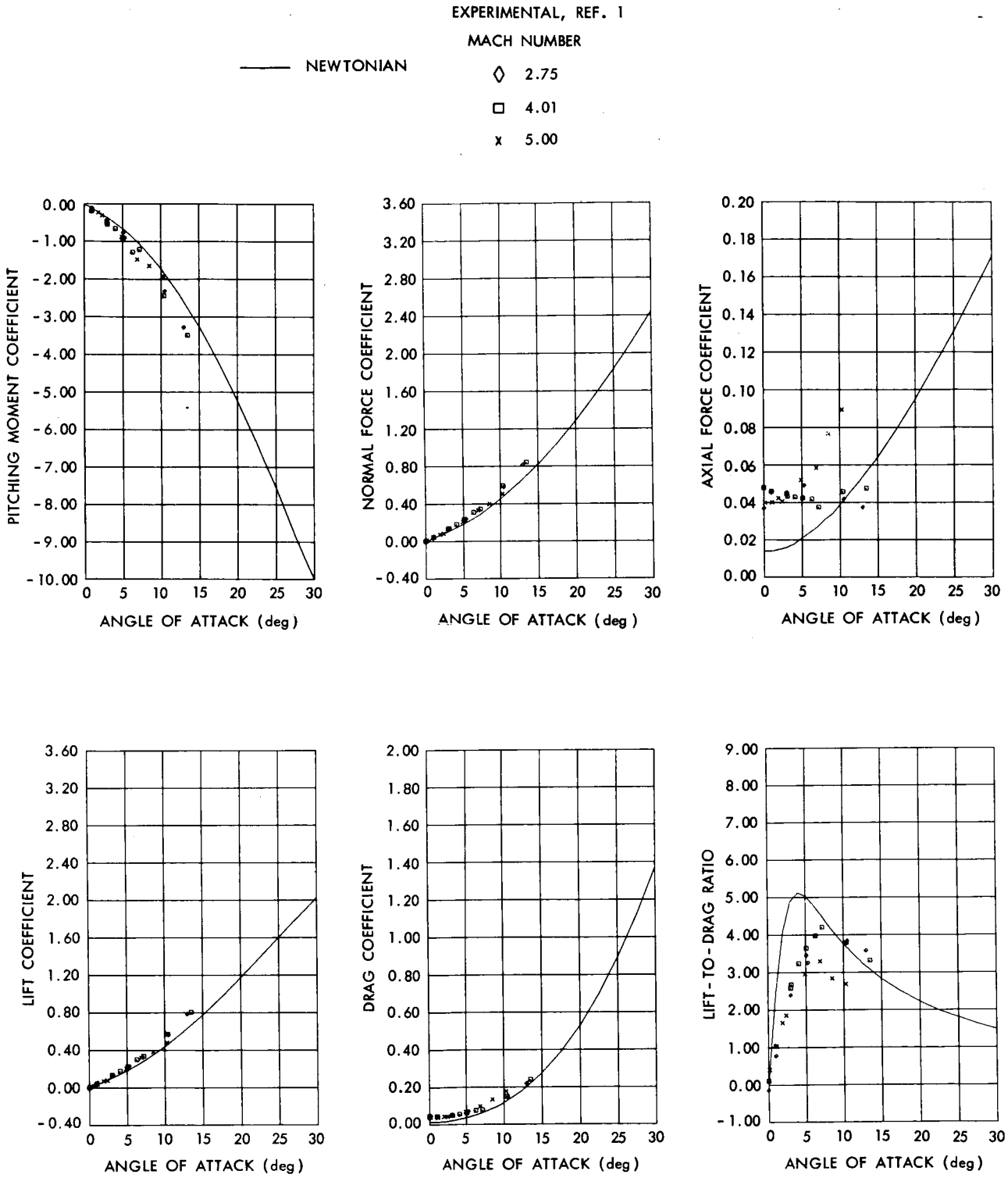

(c) f = 7

Figure 4–Comparison of theoretical and experimental aerodynamic characteristics of fineness ratio 3, 5 and 7 tangent ogive bodies.